

Influence of bond valence on microwave dielectric properties of (1-x)CaWO₄-xLnNbO₄ (Ln=Nd, Sm) solid solutions

Eung Soo Kim · Soon Ho Kim

Published online: 29 March 2007
© Springer Science + Business Media, LLC 2007

Abstract Microwave dielectric properties of (1-x)CaWO₄-xLnNbO₄ (Ln=Nd, Sm) ceramics were investigated as a function of LnNbO₄ content ($0.05 \leq x \leq 0.30$). Solid solutions with scheelite structure were obtained with LnNbO₄ content up to $x=0.3$ of Ln=Nd and/or $x=0.2$ of Ln=Sm, respectively. The unit-cell volume was decreased with the increase of B-site bond valence. For the solid solutions, dielectric constant (K) was slightly increased with LnNbO₄ content and K of the specimens with NdNbO₄ was higher than that of SmNbO₄. This result was due to the larger dielectric polarizability of NdNbO₄ (17.02 Å) than SmNbO₄ (16.75 Å). The quality factor (Qf) was dependent on the microstructure of the specimens. Temperature coefficient of resonant frequency (TCF) increased with the increase of LnNbO₄ content due to the decrease of the differences between A-site and B-site bond valence in ABO₄ scheelite.

Keywords CaWO₄-LnNbO₄ (Ln=Sm, Nd) · Microwave dielectric properties · Bond valence · Dielectric polarizability

1 Introduction

High performance and compactness of electronic devices have been required with the rapid progress of electronic industry, and largely depended on the integrations of materials with good electrical properties as electronic passive components compatible with the electronic circuit design.

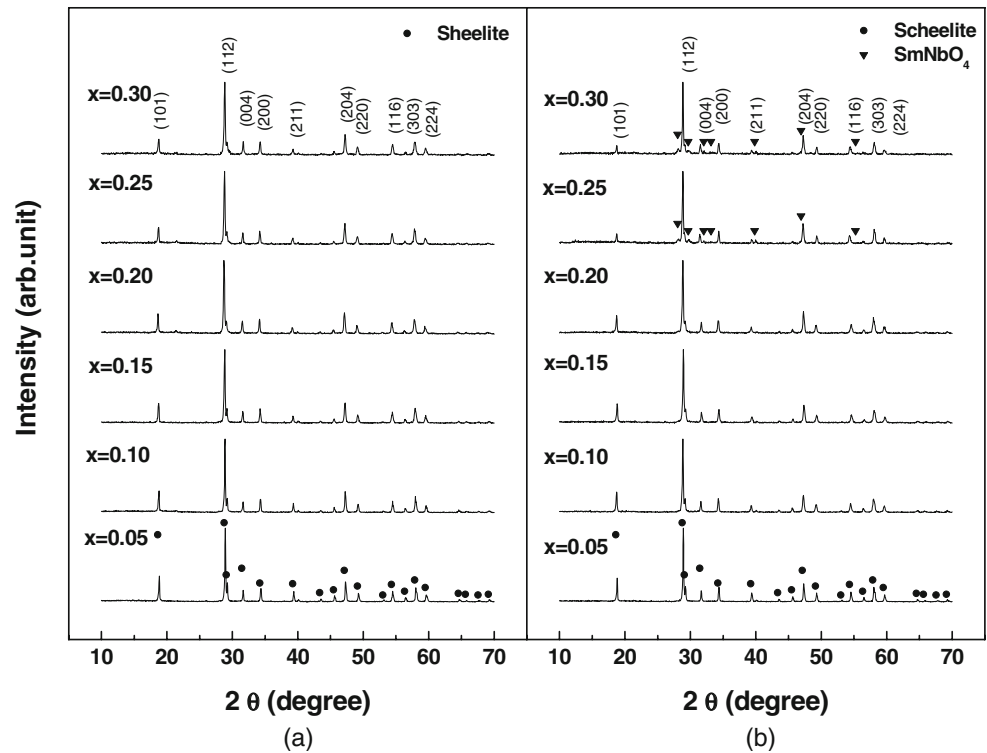
These integration activities will be accelerated to System-On-Chip (SOC) and System-In-Package (SIP) technologies and the working frequencies will be higher (3G Mobile (2.5 GHz), Bluetooth (2.5 GHz), GPS (12.6 GHz), LMDS (24~40 GHz), Automotive (77 GHz)). Due to the remarkable developments of IC technologies, the active components can be reduced the size of submicron (<0.135 μm) level, however, the chip sizes of discrete R-L-C passive components are mm level. The passive components ratios to active components are 14:1–31:1 for selected portable devices required the size and weight reduction and battery powder. For an example of single board computer, these passives, 77% capacitors and resistors compared to 5% ICs, are typical bottle-neck to the development of SOC and SIP technologies [1].

At present, the integral multilayer technologies such as multilayer low-temperature co-fired ceramics (LTCC) and multilayer ceramic integrated circuits (MCIC) are promising technologies for design flexibility and optimized integration, thus being studied actively to achieve complete SOC and SIP solutions, in which not only provide an excellent platform to mix analog, digital and RF technologies but also provide hermetic packages as part of the basic interconnect structure [2, 3].

Although LTCC and MCIC technologies had demonstrated feasible achievements, these technologies are still restrictive for the integrations of passive components due to the absence of various ceramics with good microwave dielectric properties. In view of materials aspect, the dielectric properties of ceramics are strongly dependent on the composition of ceramics, the chemical nature of constituent ions, the distance between cations and anions and the structural characteristics originating from the bonding type as well as processing variables [4], therefore the relationship between the dielectric properties and the crystal structure should be addressed to predict and control

E. S. Kim (✉) · S. H. Kim
Department of Materials Engineering, Kyonggi University,
Suwon 442-760, South Korea
e-mail: eskim@kyonggi.ac.kr

Fig. 1 X-ray diffraction patterns of $(1-x)\text{CaWO}_4\text{-}x\text{LnNbO}_4$ specimens sintered at 1150 °C for 3 h; **(a)** Ln=Nd, **(b)** Ln=Sm



the microwave dielectric properties of ceramics, and to search the new microwave dielectrics available to the passive integration technologies effectively.

Based on these considerations, it could be expected that the control of microwave dielectric properties could be achieved by the structural modifications with oxygen polyhedra, which can be effectively evaluated by a bond valence because the bond valence is a function of bond length and bond strength between cation and anion [5]. In this study, the dependence of microwave dielectric properties of $(1-x)\text{CaWO}_4\text{-}x\text{LnNbO}_4$ (Ln=Nd, Sm) ceramics ($0.05 \leq x \leq 0.30$) on the modifications of crystal structure were investigated by the evaluation of A- and/or B- site bond valence in ABO_4 with scheelite structure.

2 Experimental procedure

$(1-x)\text{CaWO}_4\text{-}x\text{LnNbO}_4$ (Ln=Nd, Sm) ceramics ($0.05 \leq x \leq 0.30$) were prepared by a conventional solid-state reaction from reagent grade powders of CaCO_3 , Nd_2O_3 , Sm_2O_3 , WO_3 and Nb_2O_5 . The powders were separately prepared according to the desired stoichiometric CaWO_4 and LnNbO_4 (Ln=Nd, Sm) and ground in ethyl alcohol for 24 h in a ball mill with ZrO_2 balls. Prepared powders of CaWO_4 and LnNbO_4 (Ln=Nd, Sm) were dried and calcined at 700 °C for 3 h, and 1100 °C for 3 h, respectively. The calcined powders were mixed according to the mole fraction $(1-x)\text{CaWO}_4\text{-}x\text{LnNbO}_4$ (Ln=Nd, Sm) and ground again in a ball-mill, and then cold-isostatically

Table 1 Bond valence of $(1-x)\text{CaWO}_4\text{-}x\text{LnNbO}_4$ (Ln=Nd, Sm) specimens sintered at 1150 °C for 3 h.

Ln	x	$R_{\text{A-O}}$	4 ($d_{\text{A-O}}$)	2 ($d_{\text{A-O}}$)	2 ($d_{\text{A}''\text{-O}}$)	V_{A}	$R_{\text{B-O}}$	4 ($d_{\text{B-O}}$)	V_{B}	$V_{\text{B}} - V_{\text{A}}$
Nd	0.05	1.9745	2.4216	2.4979	2.6523	2.0008	1.9205	1.7378	6.5547	4.5539
	0.10	1.9820	2.4212	2.5081	2.6615	2.0219	1.9200	1.7397	6.5119	4.4900
	0.15	1.9895	2.4230	2.5112	2.6645	2.0505	1.9195	1.7412	6.4758	4.4253
	0.20	1.9970	2.4286	2.5180	2.6716	2.0581	1.9190	1.7455	6.3933	4.3352
	0.25	2.0045	2.4324	2.5186	2.6728	2.0852	1.9185	1.7475	6.3494	4.2642
	0.30	2.0120	2.4320	2.5226	2.6764	2.1207	1.9180	1.7482	6.3298	4.2091
Sm	0.05	1.9731	2.4528	2.4806	2.6419	1.9293	1.9205	1.7497	6.3466	4.4173
	0.10	1.9791	2.4487	2.4794	2.6402	1.9767	1.9200	1.7474	6.3776	4.4009
	0.15	1.9852	2.4473	2.4788	2.6394	2.0150	1.9195	1.7466	6.3829	4.3679
	0.20	1.9912	2.4455	2.4786	2.6389	2.0548	1.9190	1.7456	6.3910	4.3362

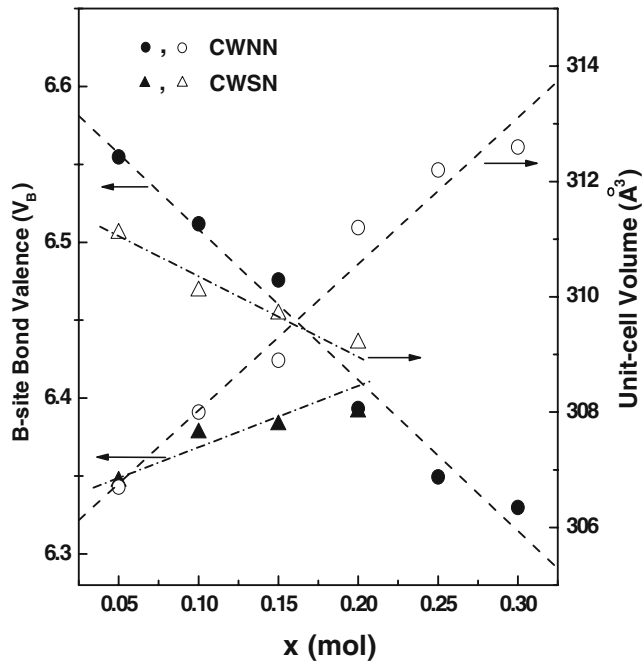


Fig. 2 Unit-cell volume and B-site bond valence (V_B) of $(1-x)\text{CaWO}_4\text{-}x\text{LnNbO}_4$ ($\text{Ln}=\text{Nd}, \text{Sm}$) specimens sintered at $1150\text{ }^\circ\text{C}$ for 3 h

pressed at $1,500\text{ kg/cm}^2$. These disks were sintered from $1150\text{ }^\circ\text{C}$ for 3 h.

Powder X-ray diffraction analysis (D/Max-3C, Rigaku, Japan) was used to determine the crystalline phases in the calcined and the sintered specimens. Lattice parameters of the sintered specimens were determined from the X-ray diffraction patterns (Fig. 1) by the least square method [8]. Polished surfaces of the sintered specimens were observed using scanning electron microscopy (JSM, 6500F, JEOL, Japan). The dielectric constant, unloaded Q value at frequencies of 9–10 GHz were measured by the post resonant method developed by Hakki and Coleman [9].

Table 2 Physical properties of $(1-x)\text{CaWO}_4\text{-}x\text{LnNbO}_4$ ($\text{Ln}=\text{Nd}, \text{Sm}$) specimens sintered at $1150\text{ }^\circ\text{C}$ for 3 h.

Ln	x (mol)	Lattice parameter (Å)		Unit-cell volume (Å^3)	Apparent density (g/cm^3)	Relative density (%)
		a	c			
Nd	0.05	5.1321	11.6437	306.7	6.0425	96.8
	0.10	5.1239	11.7317	308.0	6.0586	97.3
	0.15	5.1270	11.7501	308.9	6.0504	97.3
	0.20	5.1382	11.7858	311.2	6.0535	98.0
	0.25	5.1486	11.7761	312.2	6.0274	97.7
	0.30	5.1447	11.8116	312.6	6.0313	97.8
Sm	0.05	5.2305	11.3732	311.1	6.0921	99.0
	0.10	5.2198	11.3802	310.1	6.0760	98.2
	0.15	5.2164	11.3799	309.7	6.0814	98.1
	0.20	5.2114	11.3858	309.2	6.0905	97.9

TCF was measured by the cavity method [10] at frequencies of 9–10 GHz and the temperature range of $25\sim 80\text{ }^\circ\text{C}$.

The observed dielectric polarizability ($\alpha_{\text{obs.}}$) was obtained from the Clausius–Mossotti equation and the unit-cell volume, and theoretical dielectric polarizability ($\alpha_{\text{theo.}}$) of the specimens was calculated from the ionic polarizabilities of composing ions and the additivity rule of dielectric polarizabilities, respectively, [11, 12].

The bond valences between A-, or B-site cation and oxygen ion, $v_{(A,B,-O)}$ were calculated from Eq. 1 [13].

$$v_{(A,B,-O)} = \exp \left[\frac{(R_{(A,B,-O)} - d_{(A,B,-O)})}{b'} \right] \quad (1)$$

where, $R_{(A,B,-O)}$ is the bond valence parameter, $d_{(A,B,-O)}$ is the bond length between A-, or B-site cation and oxygen ion, and b' is commonly taken to be a universal constant equal to 0.37 \AA [14]. The bond valence parameters followed the values in the previous report [13]. For the scheelite of tetragonal structure, A-, and B-site bond valences with coordination number of 8 and 4, V_A , and V_B were calculated from Eqs. 2 and 3, respectively.

$$V_A = 8 \times v_{(A-O)} \quad (2)$$

$$V_B = 4 \times v_{(B-O)} \quad (3)$$

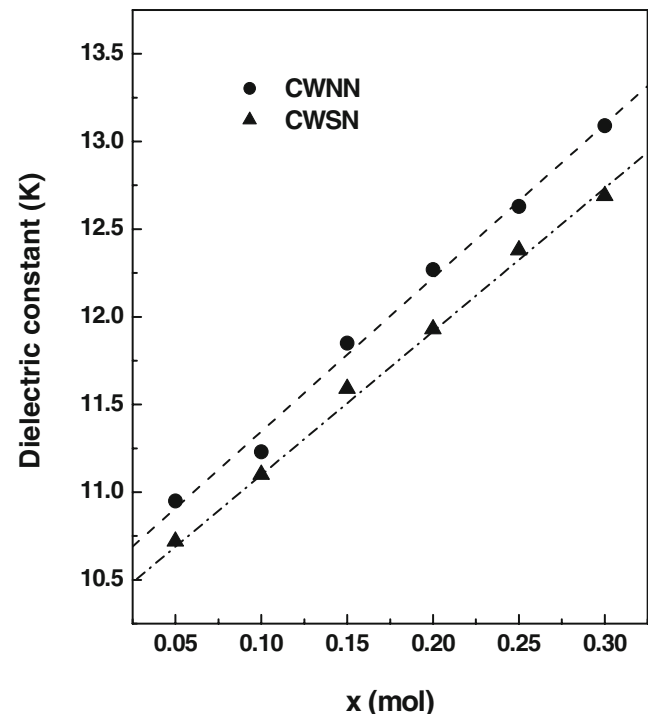


Fig. 3 Dielectric constant of $(1-x)\text{CaWO}_4\text{-}x\text{LnNbO}_4$ ($\text{Ln}=\text{Nd}, \text{Sm}$) specimens sintered $1150\text{ }^\circ\text{C}$ for 3 h

Table 3 Theoretical and observed polarizabilities of (1-x) CaWO₄-xLnNbO₄ (Ln=Nd, Sm) specimens sintered at 1150 °C for 3 h.

Ln	x (mol)	Theoretical $\alpha_{theo.}$	Observed				$\Delta(\%)$ $(\alpha_{obs} - \alpha_{theo.})/\alpha_{obs.} \times 100$
			K	$V_{unit-cell}$	Z	$\alpha_{obs.}$	
Nd	0.05	14.4645	10.95	306.7	4	14.0633	-2.8531
	0.10	14.5990	11.23	308.0	4	14.2144	-2.7055
	0.15	14.7335	11.85	308.9	4	14.4411	-2.0249
	0.20	14.8680	12.27	311.2	4	14.6667	-1.3725
	0.25	15.0025	12.63	312.2	4	14.8104	-1.2971
	0.30	15.1370	13.09	312.6	4	14.9492	-1.2564
Sm	0.05	14.4510	10.72	311.1	4	14.1906	-1.8353
	0.10	14.5720	11.10	310.1	4	14.2675	-2.1344
	0.15	14.6930	11.59	309.7	4	14.4019	-2.0213
	0.20	14.8140	11.93	309.2	4	14.4808	-2.3009

3 Results and discussion

It has been reported [6] that CaWO₄ with scheelite structure shows the phase transition from tetragonal to monoclinic with temperature and pressure, and the monoclinic structure of A³⁺B⁵⁺O₄ (A=lanthanides ion, B=Nb, Ta) is a distortion of A²⁺B⁶⁺O₄ with scheelite structure, which is called fergusonite. Also, the compounds of scheelite and fergusonite structure were formed the solid solutions into scheelite structure [7]. From the XRD patterns of CaWO₄-NdNbO₄ (CWNN) system, a single phase with tetragonal scheelite structure was obtained and well crystallized through the entire composition range, however, SmNbO₄ with fergusonite structure was detected as a secondary phase above x=0.25 in (1-x)CaWO₄-xSmNbO₄ (CWSN) system.

Considering larger differences of B-site ionic radii (0.06 Å for both CWNN and CWSN) than those of A-site (0.011 Å for CWNN, 0.041 Å for CWSN) [13], the changes of unit-cell volume could be effectively explained by B-site bond valence of ABO₄ solid solutions. To obtain the B-site bond valence, the interatomic distances (d_{B-O}) between W, Nb and O were calculated from the lattice parameters obtained from XRD patterns by the least square method, as follows;

$$d_{B-O} = \sqrt{(0.241 \times a)^2 + (0.151 \times a)^2 + (0.162 \times c/2)^2} \tag{4}$$

where, *a* and *c* are the lattice parameters of *a* and *c*-axes in tetragonal scheelite, respectively. The interatomic distance between W, Nb and O for CaWO₄-NdNbO₄ (CWNN) system increased, while those for CaWO₄-xSmNbO₄ (CWSN) system decreased, which in turn, the B-site bond valences of CWNN decreased from 6.5547 Å (*x*=0.05) to 6.3298 Å (*x*=0.30), and those of CWSN increased from 6.3466 Å (*x*=0.05) to 6.3910 Å (*x*=0.20). (Table 1) Finally, the unit-cell volume of CWNN was increased, while that of CWSN was decreased with an increase of LnNbO₄ content,

as shown in Fig. 2. Some of the physical properties data are listed in Table 2.

Figure 3 shows the dielectric constant of CaWO₄-LnNbO₄ (Ln=Nd, Sm) ceramics sintered at 1150 °C for 3 h. At microwave frequency, dielectric constant is dependent on the ionic polarizability, density and secondary phase of the specimens [15]. For the solid solutions of CaWO₄-LnNbO₄ (Ln=Nd, Sm), the dielectric constant (K) was largely depended on the dielectric polarizabilities because the relative density was above 96% and there were no secondary phase. Due to the larger dielectric polariz-

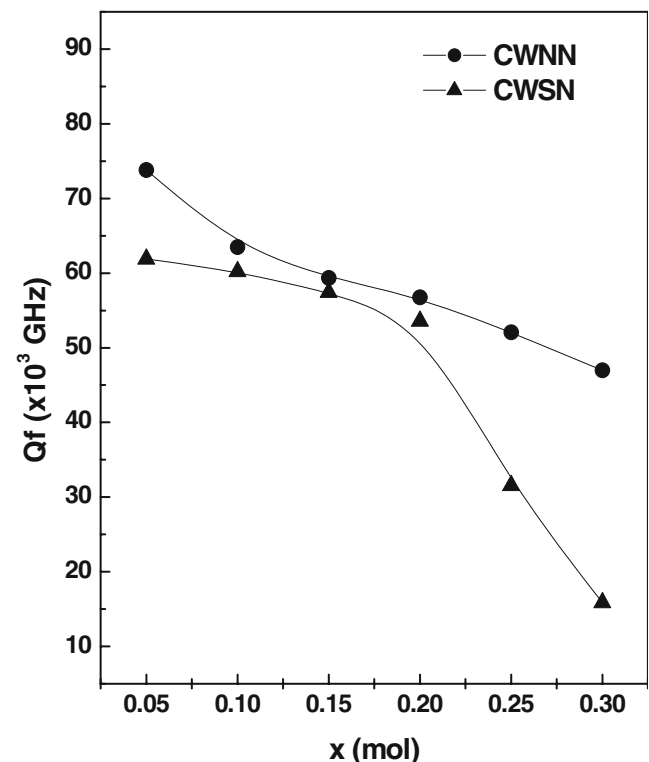


Fig. 4 Quality factor (Qf) of (1-x)CaWO₄-xLnNbO₄ (Ln=Nd, Sm) specimens sintered at 1150 °C for 3 h

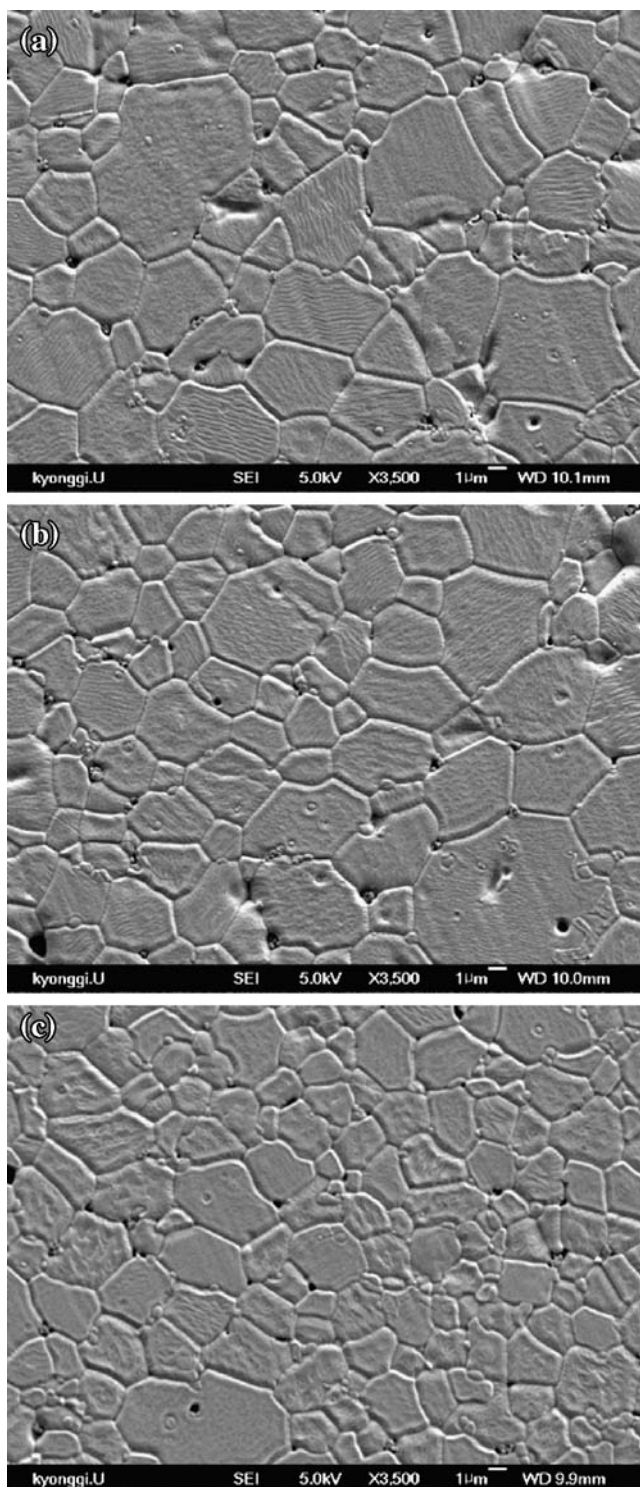


Fig. 5 SEM photographs of $(1-x)\text{CaWO}_4\text{-}x\text{NdNbO}_4$ specimens sintered at $1150\text{ }^\circ\text{C}$ for 3 h; (a) $x=0.10$, (b) $x=0.20$, (c) $x=0.30$

ability of NdNbO_4 (17.02 \AA) [11] than SmNbO_4 (16.75 \AA) [11], CWNN system showed larger value of dielectric constant than that of CWSN system. Also the dielectric constant of the specimens was increased with LnNbO_4

content because the dielectric polarizabilities of LnNbO_4 were larger than CaWO_4 (14.33 \AA) [11].

As shown in Table 3, the theoretical ($\alpha_{\text{theo.}}$) and the observed dielectric polarizabilities ($\alpha_{\text{obs.}}$) increased with increasing LnNbO_4 ($\text{Ln}=\text{Nd}, \text{Sm}$) content due to the larger dielectric polarizability of LnNbO_4 than CaWO_4 . In general, the theoretical polarizabilities ($\alpha_{\text{theo.}}$) calculated by the additivity rule of dielectric polarizability was higher than the observed value ($\alpha_{\text{obs.}}$) obtained from the measured dielectric constant because most of the polarizabilities of each ion were derived from single crystal dielectric data [12]. Also, the deviations of $\alpha_{\text{obs.}}$ from $\alpha_{\text{theo.}}$ were decreased with NdNbO_4 content, while those were increased with SmNbO_4 content. These results are due to the different changes of unit-cell volume with the kind of lanthanide ion in LnNbO_4 ($\text{Ln}=\text{Nd}, \text{Sm}$) as shown in Fig. 2, which is corresponded to the different trend of the B-site bond valence changes in ABO_4 sheelite compound.

Figure 4 shows the quality factor (Qf) of $(1-x)\text{CaWO}_4\text{-}x\text{LnNbO}_4$ ($\text{Ln}=\text{Nd}, \text{Sm}$) ceramics sintered at $1150\text{ }^\circ\text{C}$ for 3 h. It is reported that Qf values are strongly depended on the density, impurity, secondary phase and grain size [16]. The effect of density on the Qf value of $\text{CaWO}_4\text{-LnNbO}_4$ ceramics, which showed a higher relative density than 96%, could be neglected because the Qf value was independent of relative density greater than 90% [17]. For the specimens with NdNbO_4 (CWNN), the effect of impurity and secondary phase on the Qf value could also be neglected because

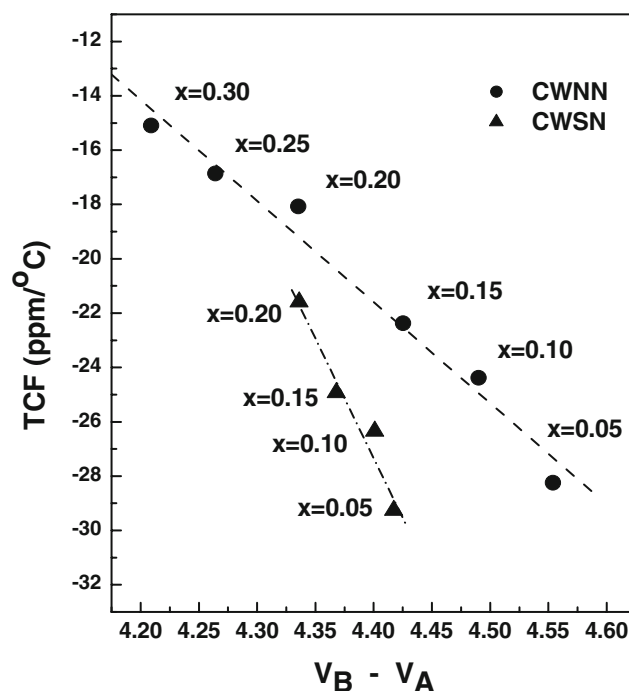


Fig. 6 TCF and the relative difference of A- and B-site bond valences of $(1-x)\text{CaWO}_4\text{-}x\text{LnNbO}_4$ ($\text{Ln}=\text{Nd}, \text{Sm}$) specimens sintered at $1150\text{ }^\circ\text{C}$ for 3 h

there was no impurity and secondary phase, as confirmed in Fig. 1. Therefore the decrease of Qf value with NdNbO₄ content could be attributed to the increase of grain size, as shown in Fig. 5. The grain size of CWNN was decreased with NdNbO₄ content. Similar tendency was observed for the specimens with SmNbO₄. For the specimens with SmNbO₄ (CWSN), Qf value was slightly decreased with SmNbO₄ content up to $x=0.20$, and then decreased remarkably due to the formation of secondary phase, SmNbO₄ which has a lower Qf value (6,500 GHz) than CWSN solid solutions.

Generally, the temperature coefficient of resonant frequency (TCF) is mainly related to the temperature dependence of dielectric constant (TCK) which depended on the recovery energy of structural distortion of oxygen polyhedra. Even though the degree of structural distortion can be evaluated by the bond valence [13], the structural distortions are too complicate to evaluate for some crystal systems, especially for solid solutions, and thus the effect of structural distortion on TCF can be evaluated by all of cation bond valences, which has a unique bond valence depending on crystal structure. For ideal tetragonal scheelite ABO₄ with no structural distortion, A- and B-site bond valence should be +2 and +6, respectively. Therefore, the structural distortion of oxygen polyhedra can be effectively evaluated by the relative differences of A- and B-site bond valences.

As shown in Fig. 6, TCF is strongly depended on the relative differences of A- and B-site bond valences. With the increase of LnNbO₄ (Ln=Nd, Sm) content, the relative differences of A- and B-site bond valences were decreased, which is corresponded to the decrease of structural distortion of oxygen polyhedra. Therefore, TCF of CaWO₄-LnNbO₄ (Ln=Nd, Sm) ceramics was increased with LnNbO₄ content.

4 Conclusion

For the specimens of $(1-x)\text{CaWO}_4\text{-}x\text{LnNbO}_4$ (Ln=Nd, Sm; $0.05 \leq x \leq 0.30$) sintered 1150 °C for 3 h, a single phase with tetragonal scheelite structure was detected up to $x=0.30$ of Nd and $x=0.20$ of Sm, respectively. In the solid solution range, B-site bond valence of the specimens with

NdNbO₄ was decreased, while that with SmNbO₄ was increased. These results are due to the different changes of unit-cell volume with the kind of lanthanide ion in LnNbO₄ (Ln=Nd, Sm).

With the increase of LnNbO₄ content, the dielectric constant was increased, and the specimens with NdNbO₄ showed a larger dielectric constant than those with SmNbO₄, which was due to the larger ionic polarizabilities of Nd than that of Sm. The quality factor (Qf) was dependent on the grain size as well as the secondary phase. The temperature coefficient of resonant frequency was dependent on the relative differences of A- and B-site bond valences, and increased with LnNbO₄ content.

Acknowledgements This work was supported by LG Innotek and the Ministry of Commerce, Industry and Energy.

References

1. *The NEMI Roadmap: Integrated Passives Technology and Economics*. Proc. of the Capacitor and Resistor Technology Symposium (CARTS), Scottsdale, AZ, April 2003
2. A. Sutono, A. Pham, J. Laskar, W.R. Smith, IEEE RFIC-S 175, (1999)
3. K. Delaney, J. Barrett, J. Barton, R. Doyle, IEEE Trans. Adv. Packaging **22**, 78 (1999)
4. E.S. Kim, B.S. Chun, Jpn. J. Appl. Phys. **43**, 219 (2004)
5. N.B. Brese, M. O'Keefe, Acta Crystallogr. **B47**, 192 (1991)
6. K. Ezaki, Y. Baba, H. Takahashi, K. Shibata, S. Nakano, Jpn. J. Appl. Phys. **32**, 4319 (1993)
7. D. Errandonea, F.J. Manjón, M. Somayazulu, D. Häusermann, J. Solid State Chem. **177**, 1087 (2004)
8. M.U. Cohen, Rev. Sci. Instrum. **6**, 68 (1935)
9. B.W. Hakki, P.D. Coleman, IRE Trans. Microwave Theor. Tech. **MTT-8**, 402 (1960)
10. T. Nishikawa, K. Wakino, H. Tanaka, Y. Ishikawa, IEEE MTT-S Int. Microwave Symp. Dig. **3**, 277 (1987)
11. R.D. Shannon, J. Appl. Phys. **73**, 348 (1993)
12. R.D. Shannon, M.A. Subramanian, Phys. Chem. Miner. **16**, 747 (1989)
13. R.D. Shannon, Acta Crystallogr. **A32**, 751 (1976)
14. I.D. Brown, D. Altermatt, Acta Crystallogr. **B41**, 244 (1985)
15. E.S. Kim, B.S. Chun, K.H. Yoon, Mater. Sci. Eng., B **99**, 93 (2003)
16. W.S. Kim, E.S. Kim, K.H. Yoon, J. Am. Ceram. Soc. **82**, 2111 (1999)
17. D.M. Iddles, A.J. Bell, A.J. Moulson, J. Mater. Sci. **27**, 6303 (1992)